Eur. Phys. J. A **13**, 363–376 (2002)

THE EUROPEAN PHYSICAL JOURNAL A

Radiative transitions in mesons in a non-relativistic quark model

R. Bonnaz, B. Silvestre-Brac[a], and C. Gignoux

Institut des Sciences Nucléaires, 53 Av. des Martyrs, F-38026 Grenoble Cedex, France

Received: 16 October 2001 / Revised version: 10 December 2001
Communicated by P. Schuck

Abstract. In the framework of the non-relativistic quark model, an exhaustive study of radiative transitions in mesons is performed. Emphasis is placed on several points. Some traditional approximations (long-wavelength limit, non-relativistic phase space, dipole approximation for $E1$ transitions, Gaussian wave functions) are analyzed and their effects commented. A complete treatment using three different types of realistic quark-antiquark potential is made. The overall agreement with experimental data is quite good, but some improvements are suggested.

PACS. 14.40.-n Mesons – 13.40.Hq Electromagnetic decays – 12.39.Jh Nonrelativistic quark model

1 Introduction

Quantum Chromodynamics (QCD) is today the only reliable theory for describing strong interactions. There exist many systems that can be used as a laboratory for exploring and testing the properties of this basic theory. Among them, the meson and baryon sectors have been subjected to a lot of investigation, essentially because they are very easily produced. However they belong to the non-perturbative application of QCD and thus are not easily described starting from first principles. Despite many improvements in recent years, on both theoretical and computational sides, the lattice gauge calculations are still not completely reliable and cannot explain the full set of known properties, even for the simplest systems such as the mesons, which consist of a valence quark-antiquark pair.

This explains why so many phenomenological approaches have been developed in order to describe the non-perturbative part of QCD. Among them the non-relativistic quark model (NRQM) has met with an impressive number of successes [1]. The puzzling question is that it still works even in situations where it is expected to fail; there exist certainly some deep reasons for such a behaviour although they have not yet been clarified precisely (see [2]). Basically the NRQM needs to solve a Schrödinger type equation with two-body quark-quark (or quark-antiquark) interactions. In recent years, the determination of the interaction between constituent quarks has reached a high degree of sophistication and the whole spectra of mesons, for instance, can be accounted for in a rather satisfactory way [3,4].

[a] e-mail: silvestre@isn.in2p3.fr

The description of the spectra is a necessary but not a sufficient condition for aiming at a good explanation of non-perturbative QCD. In particular, very different potentials can give rise to spectra of the same quality. One needs other observables in order to test more precisely the resulting wave functions. A possibility is the study of static properties, such as magnetic moments or mean square radii of charge distributions. More sensitive observables concern the transitions between various states or production mechanisms (which depend essentially on the same dynamical operators). One can think, for instance, of meson decays under strong forces (a resonance giving two or several mesons) or the decays under electroweak forces (a resonance producing a photon or leptons in the final channel). The advantage of this last kind of transition is that the transition operator is known perfectly well and thus it is easier to disentangle the effects coming from less well-known strong interactions through the meson wave function ([5]).

In fact this statement is not completely true in the NRQM. Being a phenomenological theory, NRQM deals with effective degrees of freedom, the constituent quarks, and a pure Dirac form of the quark-photon vertex in the transition operator is questionable. Moreover, even in the traditional approach of radiative transitions (decay of a resonance into a resonance of lower energy plus a real photon) several types of approximations are of current use; the effect of these approximations can hide the necessity of using a more sophisticated vertex for the quark-photon coupling. Most of those approximations originate from the formulae widely used in atomic or nuclear physics which are simply translated to the meson sector. Examples are the dipole approximation for $E1$ transitions, the long-

wavelength approximation (LWLA) and a non-relativistic phase space factor.

Although these approximations are fully justified in atomic or nuclear physics, it is not obvious that they continue to work when applied to mesons. Indeed, in this sector the transition energy is typically $E_\gamma = k_\gamma = 0.1$–$0.5$ GeV, while the size of the source is roughly $R = 0.5$–1 fm $= 2.5$–5 GeV^{-1}, so that the long-wavelength condition $k_\gamma R \ll 1$ is not really justified. Comparing the photon energy to the mass of the emitting meson also convinces us that a non-relativistic phase space is probably not appropriate. Moreover the fact that the electrons in an atom or the nucleons in a nucleus have the same mass is not true in the case of some mesons, and new phenomena can appear.

During the seventies and eighties, a lot of work has been performed on radiative transitions for mesons (and also for baryons but we are less interested in this sector here). At the very beginning they were studied in the vector dominance model [6,7]. The quark model was then introduced either in the framework of the MIT bag model [8–10], the non-relativistic quark model [11–13], the 2-body Dirac equation [14–16] or some relativistic phenomenological quark models [17,18]. Unfortunately even in the most complete and nice works, as [17] or [13], there is always an approximation or an inconsistency which plagues the results or precludes precise conclusions. Up to now, there does not exist a consensus concerning "relativistic" models for two-body problems; some of them are not fully covariant (relativized quark model [17], Salpeter equations [19], two-body Dirac potentials [20], bag models [21],...), other are covariant in their formulation (Bethe-Salpeter [22], light cone dynamics [23],...) or can be considered as approximations of the Bethe-Salpeter equation (quasi-potential [24], instantaneous approximation [25],...). None of them is really free from difficulties, and the present state of art is such that none can pretend to be the ultimate relativistic theory. In particular, most of relativistic models suffer from a bad treatment of the center of mass and the relativized models do not treat with equal care the quark-quark potential and the electromagnetic operator. Before introducing relativistic effects, we believe that we should first explore in detail the NRQM, but in the best possible way. In many papers, a non-relativistic phase space or a long-wavelength approximation are used and we will see that this is not justified in the meson sector. In addition, only very few studies consider the totality of the known experimental data but instead focus on very specific transitions (light quark sector or heavy quark sector or even more restricted sets).

The aim of this paper is to present an exhaustive study of radiative transitions, in the framework of NRQM, avoiding the various approximations widely employed in the literature and using wave functions consistent with a good description of the meson spectra. Our philosophy is that spectra and transitions rely on the same dynamics and cannot be separated. Thus, we base our analysis on 3 different quark-quark potentials giving a good description of the resonance energies; the resulting wave functions are introduced as such in the calculation of transition widths, so that all our results are *parameter free*. A comparison between them is highly instructive. In particular, we have in mind to see whether it is necessary to modify the quark-photon vertex; our study is thus a necessary first step before undertaking a more difficult and ambitious program, which is beyond the scope (both theoretically and numerically) of the present work.

In this paper, we will consider all the radiative transitions (which are sufficiently reliable) that are reported in the particle data group booklet because we aim at an exhaustive analysis. The experimental data can be gathered into several groups:

- the transitions allowed by LWLA; they are essentially $M1$ transitions ($^3S_1 \to {}^1S_0$ or $^1S_0 \to {}^3S_1$) and $E1$ transitions ($^3P_J \to {}^3S_1$ or $^3S_1 \to {}^3P_J$); there is also the particular $E1$ transition corresponding to the decay $b_1(1235) \to \pi\gamma$ ($^1P_1 \to {}^1S_0$);
- the transitions forbidden by LWLA; they are scarce but interesting : they correspond to $^3P_J \to {}^1S_0$, $^3S_1 \to {}^3S_1$ and $^1P_1 \to {}^3S_1$ transitions.

The paper is organized as follows. In the next section, we show how the meson wave functions are obtained and also present the different quark-antiquark potentials that we are studying. In the third section, we recall the formalism necessary for the description of radiative transitions putting the emphasis on the general treatment and the differences corresponding to the various approximations that we want to discuss. In sect. 4 our final expressions for the total widths are summarized. Results are presented, with a brief discussion of various approximations in sect. 5 and sect. 6 contains the conclusion.

2 Description of mesons

In the NRQM, the meson is considered as a two-particle system: a (constituent) quark of mass m_1 and an antiquark of mass m_2 submitted to a potential $V(r)$, so that the corresponding Schrödinger equation reads:

$$\left[m_1 + m_2 + \frac{\mathbf{p}^2}{2\mu} + V(r)\right] \mid \Psi_\alpha\rangle = m_\alpha \mid \Psi_\alpha\rangle\,, \qquad (1)$$

where μ is the reduced mass, $\mathbf{p}$ the relative momentum, and m_α the total mass of the resonance. This last quantity, as well as the wave function $\mid \Psi_\alpha\rangle$, of course depends on the choice for the potential. The ordinary quarks u and d can be considered as isospin doublets; they are symbolized generically as n.

2.1 The potentials

In this paper we will consider three different types of potential, the so-called AL1 and AP1 potentials [26] and the DNR potential [3]. For the purpose of our analysis, it is not necessary to introduce very sophisticated forms including

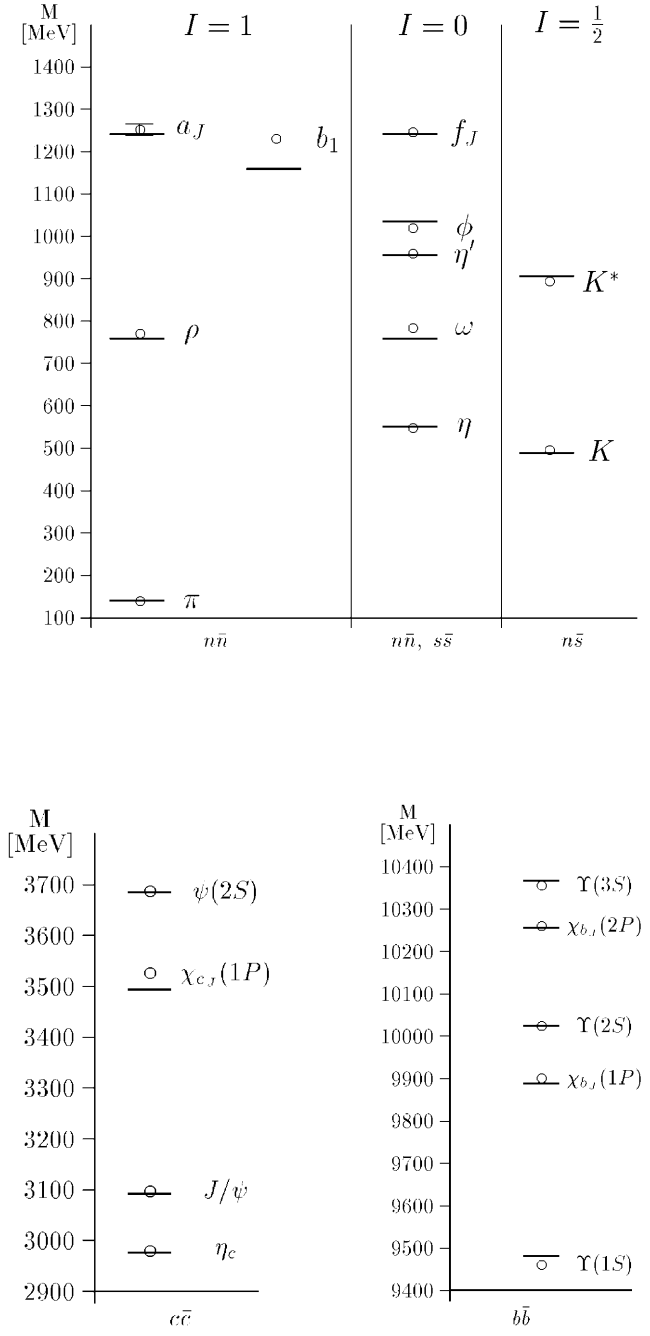

Fig. 1. Mass spectra for most of the resonances studied in this article. The open circles represent the experimental values with their error bars (the short horizontal lines) if they are significant. The large horizontal lines are the theoretical values obtained with the DNR potential.

spin-orbit, tensor forces, ...whose effects are not so important and which considerably complicate the formalism.

The first potentials, AL1 and AP1, are the simplest ones and their parameters have been fitted in order to best reproduce the meson resonances in all sectors. They both contain a central "constant+Coulombic" term (remnant of one-gluon exchange) and a hyperfine term with a Gaussian radial dependence. The peculiarity, in contrast to other usual potentials such as the one due to Bhaduri and coworkers [27], is that the range of this Gaussian term is mass dependent, following Ono's prescription [28]. The two potentials differ by the confinement term. In AL1, it behaves linearly with distance, whereas for AP1 it behaves with power 2/3, more suited for the Regge trajectories in non-relativistic dynamics. The baryon spectra are also well reproduced with those potentials. The parameters can be found in [26] and the spectra can be provided on request. Most of the resonances are correctly described but a drawback of those potentials, common to many others, is that the $|\ \Psi_{\eta_n}\rangle = |\ n\bar{n}, I = 0, L = 0, S = 0\rangle$ state is degenerate with the π and the $|\ \Psi_{\eta_s}\rangle = |\ s\bar{s}, I = 0, L = 0, S = 0\rangle$ state is unphysical. This means that the η and η' resonances do not come out correctly. Nevertheless, one can simulate their wave functions by the traditional prescription

$$|\ \Psi_\eta\rangle = \frac{1}{\sqrt{2}}[|\ \Psi_{\eta_n}\rangle - |\ \Psi_{\eta_s}\rangle]\ ,\ |\ \Psi_{\eta'}\rangle = \frac{1}{\sqrt{2}}[|\ \Psi_{\eta_n}\rangle + |\ \Psi_{\eta_s}\rangle]\ . \tag{2}$$

The DNR potential is aimed to remove this difficulty. This is achieved by introducing instanton effects. The non-relativistic reduction of instantonic terms is active only for $L = 0, S = 0$ [29]. Thus, it participates in the dynamics of pions and kaon and it introduces a coupling term between $n\bar{n}$ and $s\bar{s}$ sectors so that the η and η' wave functions are given by

$$|\ \Psi_\eta\rangle = [|\ \Psi_{\eta_n}\rangle - |\ \Psi_{\eta_s}\rangle]\ ,\ |\ \Psi_{\eta'}\rangle = [|\ \Psi_{\eta'_n}\rangle + |\ \Psi_{\eta'_s}\rangle]\ . \tag{3}$$

However, in this case the various functions Ψ_{η_n},... result from a coupled-channel calculation and cannot be considered as mixing angles; they are determined dynamically and $|\langle\Psi_{\eta_i}|\Psi_{\eta_i}\rangle|^2$ represents the probability that the resonance is found in the flavor channel $i\bar{i}$ (the signs are chosen in such a way that $|\Psi_{\eta_n}\rangle$ and $|\Psi_{\eta_s}\rangle$ have the same sign for $r \to 0$ or $r \to \infty$). Another aspect of the potential is that the short-range behaviour is fitted to the experimental values of $\alpha_s(q^2)$ and that the constituent quarks are no longer point-like but acquire a Gaussian extension. The effective potential used in the Schrödinger equation results from the convolution of the bare potential with this Gaussian density. Essentially, the Coulombic term is replaced by error functions, the linear confinement remains linear and the short-range instanton and hyperfine terms are represented by Gaussian expressions. The parameters can be found in the original paper [3]. To give an idea of the quality of the spectra concerning the resonances studied in this work, we present a comparison with experimental data in fig. 1. This potential is the most sophisticated and it describes quite nicely the entire spectrum. The Regge trajectories are also well reproduced if one considers the centroids of L-S multiplets [3].

2.2 Meson wave functions

Because of the rotational invariance, the meson wave function is written as

$$|\ \Psi_{ILSJ}\rangle = \eta_I(1,2)[\Phi_{nL}(1,2)\chi_S(1,2)]_J\ , \tag{4}$$

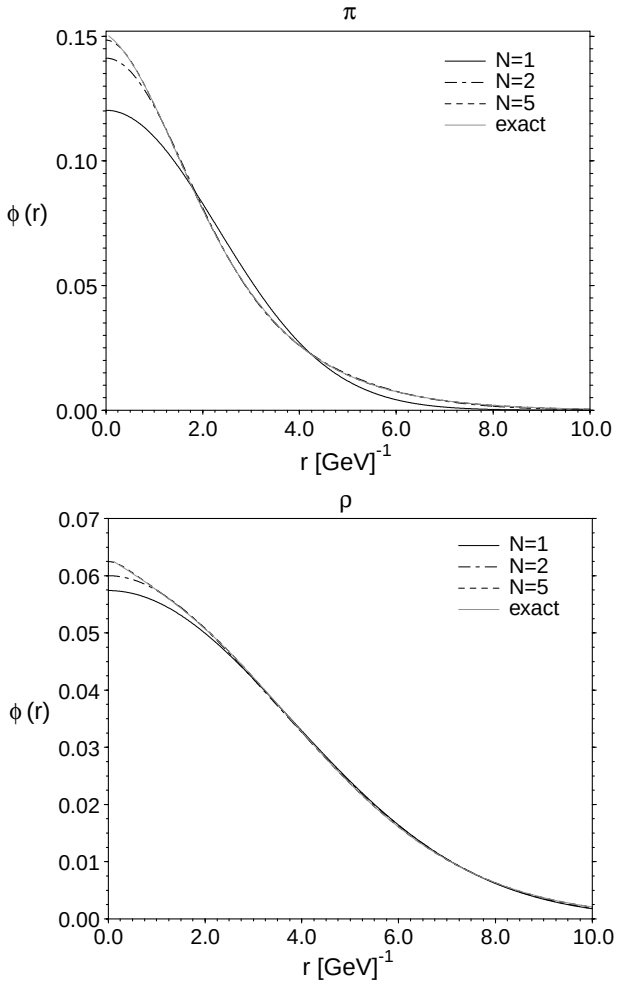

Fig. 2. π and ρ radial wave functions $\frac{R_{nL}(r)}{\sqrt{4\pi}}$ for $N = 1, 2$ and 5 Gaussian terms compared to the exact ones (obtained with AL1 potential). For $N = 5$, the curve is surimposed to the exact one.

where $\eta_I(1,2)$ is the isospin wave function with total isospin I, $\chi_S(1,2)$ is the spin wave function with total spin S and $\Phi_{nL}(1,2)$, the space wave function with orbital momentum L and radial number n. Spin S and orbital momentum L are coupled to total angular momentum J, but are nevertheless good quantum numbers. Strictly speaking, one should also include a colour wave function but it is the same for every meson and, since the transition operator does not depend on colour degrees of freedom, does not play any role. It is therefore omitted in the following. In the same way, we do not indicate the flavor content of the meson since the electromagnetic operator does not affect it; however, one should remember that the total wave function for the η resonances given by (2) or (3) is a superposition of two wave functions of type (4). The magnetic quantum numbers are not indicated here although the projection of the isospin plays a role since the operator is a mixing of isoscalar and isovector terms. We will come back to this point later on.

To deal with the matrix elements of the transition operator, we find it convenient to express the space wave function in momentum representation. Thus we put

$$\langle \mathbf{p} \mid \Phi_{nL}(1,2) \rangle = R_{nL}(p) Y_L(\hat{p}) \,. \tag{5}$$

Moreover, an approximation of the exact wave function in terms of Gaussian functions will be particularly well suited for computation of difficult quantities. We will see the various advantages of such a prescription later. In this case, we write

$$R_{nL}(p) = p^L \sum_{i=1}^{N} c_i \exp(-A_i p^2/2) \,. \tag{6}$$

In general the number of Gaussian terms needed in (6) to achieve convergence is rather small. We plot the corresponding wave functions for different values of N in fig. 2 in the case of the AL1 potential. Although there are some differences between the $N = 1$ and $N = 2$ cases, the approximation (6) can be identified very rapidly with the exact solution. In practice we perform our calculations with $N = 5$ and consider the corresponding wave function as the exact one. Thus, in the rest of the paper, we identify the wave function given by (6) with $N = 5$ with the exact wave function.

3 Radiative transitions

A number of points are already well known, and we do not want to spend too much time on them. We will focus our attention essentially on new aspects or on formulations that are discussed in detail later on. Everywhere in this paper we employ natural units $\hbar = c = 1$.

3.1 Transition operator

We begin with the non-relativistic expression of the electromagnetic transition operator between an initial meson state and a final meson state plus a real photon of momentum $\mathbf{k}$, energy $E =\mid \mathbf{k} \mid$ and polarisation $\epsilon(\mathbf{k}, \lambda)$. We adopt, as usual, the Coulomb gauge, and we normalize the plane waves in a box of volume V (as usual, α stands for the fine-structure constant).

$$H_I = -\sqrt{\frac{2\pi\alpha}{VE}} \epsilon(\mathbf{k}, \lambda) \cdot \mathbf{M} \,, \tag{7}$$

$$\mathbf{M} = \sum_{i=1}^{2} \frac{e_i}{2m_i} \exp(-i\mathbf{k} \cdot \mathbf{r}_i)(2\mathbf{p}_i - i\sigma_i \times \mathbf{k}) \,. \tag{8}$$

The summation runs over the two particles of charge e_i and mass m_i present in the meson. The first term in $\mathbf{M}$ is known as the electric term and the second one as the magnetic term. In this paper, we do not wish to consider electromagnetic modifications due to relativistic effects or to meson exchange currents, but rather to explore the consequences of a sophistication at the level of the wave function, which is more sensitive to strong interactions. With

the prescription (8), one can note that we would find the right formulae for the static magnetic moment of a punctual particle with a constituent mass m_i.

3.2 Transition amplitude

The initial meson of mass m_a is at rest and has angular momentum J_aM_a (coupling of L_a and S_a), isospin $I_aM_{I_a}$. The final meson of mass m_b has a total momentum $\mathbf{K}_b$, angular momentum J_bM_b (coupling of L_b and S_b), isospin $I_bM_{I_b}$. Inserting $\mathbf{M}$ of (8) between the corresponding wave functions (4)(in the rest frame of the meson $\mathbf{p}_1 = -\mathbf{p}_2 = \mathbf{p}$) in the momentum representation (completed by the center-of-mass plane wave), one obtains the transition amplitude

$$\mathbf{M}_{\mathrm{A}\to\mathrm{B}} = \delta_{\mathbf{K}_b,-\mathbf{k}}[\mathbf{M}^{(1)}_{\mathrm{A}\to\mathrm{B}} + \mathbf{M}^{(2)}_{\mathrm{A}\to\mathrm{B}}]\,, \tag{9}$$

$$\mathbf{M}^{(1)}_{\mathrm{A}\to\mathrm{B}} = \frac{\langle e_1\rangle}{2m_1}\int \mathrm{d}^3p\,\Phi^*_{\mathrm{B}}\left(\mathbf{p} - \frac{m_2}{m_1+m_2}\mathbf{k}\right) \times[2\mathbf{p} - i\sigma_1\times\mathbf{k}]\Phi_{\mathrm{A}}(\mathbf{p})\,, \tag{10}$$

$$\mathbf{M}^{(2)}_{\mathrm{A}\to\mathrm{B}} = \frac{\langle e_2\rangle}{2m_2}\int \mathrm{d}^3p\,\Phi^*_{\mathrm{B}}\left((\mathbf{p} + \frac{m_1}{m_1+m_2}\mathbf{k}\right) \times[-2\mathbf{p} - i\sigma_2\times\mathbf{k}]\Phi_{\mathrm{A}}(\mathbf{p})\,, \tag{11}$$

where the subscripts refer to the particle number (see fig. 3 for a graphical interpretation of quark momenta in the meson). If we use the isospin formalism $\langle e_i\rangle$ is given by formula (12), otherwise $\langle e_i\rangle$ simply means the charge corresponding to the flavor of quark i:

$$t_i = 0 : \langle e_i\rangle = e_i\,\delta_{I_aI_b}\,\delta_{M_{I_a}M_{I_b}}\,, \tag{12}$$

$$t_1 = 1/2 : \langle e_1\rangle = \delta_{M_{I_a}M_{I_b}} \times\left[\frac{1}{6}\delta_{I_aI_b} + (-1)^{I_a+t_2-1/2}\sqrt{3(I_a+1/2)} \times\langle I_aM_{I_a}10\mid I_bM_{I_b}\rangle\begin{Bmatrix}1 & 1/2 & 1/2\\ t_2 & I_a & I_b\end{Bmatrix}\right], \tag{13}$$

$$t_2 = 1/2 : \langle e_2\rangle = \delta_{M_{I_a}M_{I_b}} \times\left[-\frac{1}{6}\delta_{I_aI_b} + (-1)^{I_b+t_1-1/2}\sqrt{3(I_a+1/2)} \times\langle I_aM_{I_a}10\mid I_bM_{I_b}\rangle\begin{Bmatrix}1 & 1/2 & 1/2\\ t_1 & I_a & I_b\end{Bmatrix}\right]. \tag{14}$$

3.2.1 Long-wavelength axpproximation

Due to the recoil term in the meson B wave function, the momentum-space integral appearing in (10-11) is not easy to calculate. A widely used approximation is the long-wavelength approximation (LWLA) which consists in putting $\mathbf{k} = 0$ in the argument of Φ_{B} (this is equivalent to replacing $\exp(-i\mathbf{k}\cdot\mathbf{r})$ by 1 in coordinate representation). It is just a matter of Racah algebra to disentangle the spin and space degrees of freedom in (10-11). It is pleasing that, in this case, the electric and magnetic part, which are of different parity, cannot couple the same states; this is why we speak about electric and magnetic transitions. The electric transitions change the parity of the state, but not the spin, whereas the magnetic transitions change neither parity nor orbital momentum.

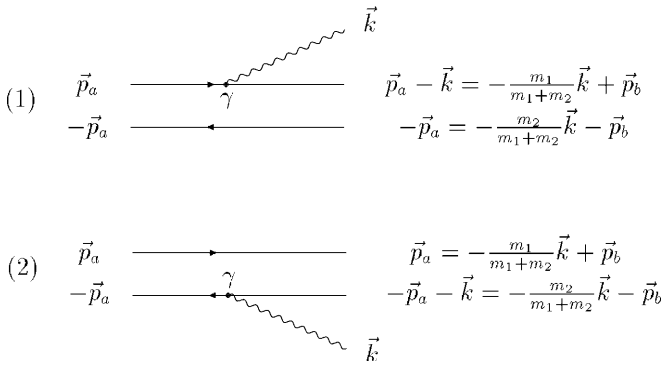

Fig. 3. Schematic representation of the elementary decay process with momentum values from the rest frame of the inital meson. (1) Denotes the emission of the real photon by the quark and gives rise to $M^{(1)}$ and (2) by the antiquark and gives rise to $M^{(2)}$. The total process amplitude is the sum of the 2 amplitudes (1) and (2).

3.2.2 Beyond long-wavelength approximation

The major advantage of using the wave functions expressed in Gaussian terms (6) is that the treatment of the general case can be dealt with rather simply. Since taking $N = 5$ is equivalent to treating the exact wave function, the following treatment solves exactly the problem. In fact, an individual term in the expansion is of the form $\Phi_L(\mathbf{p}) = \exp(-Ap^2/2)\mathcal{Y}_L(\mathbf{p})$, where $\mathcal{Y}_L(\mathbf{p}) = p^LY_L(\hat{p})$ is the usual solid harmonic. To illustrate the procedure, let us consider only one term in the expansion (one A quantity for meson A, one B quantity for meson B with a unit amplitude $c^{\mathrm{A}} = c^{\mathrm{B}} = 1$). The argument in the meson B wave function is now a linear combination of $\mathbf{p}$ and $\mathbf{k}$. Such a combination of type $\mathcal{Y}_{lm}(a\mathbf{p}_1 + b\mathbf{p}_2)$ can be easily expressed in terms of individual $\mathcal{Y}_{l_1}(\mathbf{p}_1)$ and $\mathcal{Y}_{l-l_1}(\mathbf{p}_2)$ terms. Moreover, a coupling term like $[\mathcal{Y}_{l_1}(\mathbf{p})\mathcal{Y}_{l_2}(\mathbf{p})]_{lm}$ is contracted into a single $\mathcal{Y}_{lm}(\mathbf{p})$ by well-known formulae (see *i.e.* [30]).

The same combination of $\mathbf{p}$ and $\mathbf{k}$ appearing in the exponential is a quadratic form which can be diagonalized in order to get rid of the non-diagonal terms. Let us just summarize our conclusions using some auxilliary quantities ($i = 1, 2$ refers to particle number):

$$D = \frac{A+B}{2}\,,\quad x^{(i)} = \frac{m_{3-i}B}{(m_1+m_2)(A+B)}\,,$$
$$z^{(i)} = \frac{m_{3-i}A}{(m_1+m_2)(A+B)}\,,\quad F^{(i)} = Dx^{(i)}z^{(i)}\,. \tag{15}$$

If the masses of the quark and the antiquark are the same there is no need to distinguish the quantities x, z, F and further simplifications arise which we do not wish to comment. The transition amplitudes in the general case can be converted to a more appropriate form:

$$\begin{aligned}\mathbf{M}^{(1)}_{\mathrm{A}\to\mathrm{B}} &= \frac{\langle e_1\rangle}{2m_1}\int \mathrm{d}^3q \exp(-Dq^2 - F^{(1)}k^2)\\ &\times[\mathcal{Y}^*_{L_b}(\mathbf{q} - z^{(1)}\mathbf{k})\chi_{S_b}]_{J_b}[2\mathbf{q} - i\sigma_1\times\mathbf{k}]\\ &\times[\mathcal{Y}_{L_a}(\mathbf{q} + x^{(1)}\mathbf{k})\chi_{S_a}]_{J_a}\,,\\ \mathbf{M}^{(2)}_{\mathrm{A}\to\mathrm{B}} &= \frac{\langle e_2\rangle}{2m_2}\int \mathrm{d}^3q \exp(-Dq^2 - F^{(2)}k^2)\\ &\times[\mathcal{Y}^*_{L_b}(\mathbf{q} + z^{(2)}\mathbf{k})\chi_{S_b}]_{J_b}[-2\mathbf{q} - i\sigma_2\times\mathbf{k}]\\ &\times[\mathcal{Y}_{L_a}(\mathbf{q} - x^{(2)}\mathbf{k})\chi_{S_a}]_{J_a}\,. \end{aligned} \tag{16}$$

Altough it is possible to pursue the calculations using (16), experimentally all the known transitions exhibit either $L_a = 0$ or $L_b = 0$. The resulting formulae look much simpler in those cases and we report here only these special cases since only they will be applied in the next chapter. One important difference, as compared to the LWLA, is that both the electric and magnetic terms of the operator contributes to a given transition. Let us present the result for $L_b = 0$:

$$(\mathbf{M}_{\mathrm{A}\to\mathrm{B}L_b=0})_\mu = \delta_{S_b,J_b}[\mathcal{E}_\mu(A;x) + \mathcal{M}_\mu(A;x)]\,. \tag{17}$$

The term $\mathcal{E}_\mu(A;x)$ comes from the electric part of the operator and reads

$$\begin{aligned}\mathcal{E}_\mu(A;x) &= \delta_{S_a,S_b}\frac{\sqrt{4\pi L_a}}{6}\hat{L_a}\ \Gamma(5/2)\\ &\times\langle L_a, M_a - M_b; J_b, M_b \mid J_a, M_a\rangle\\ &\times\langle 1, -\mu; L_a - 1, M_a - M_b + \mu \mid L_a, M_a - M_b\rangle\\ &\times(-1)^\mu\mathcal{Y}_{L_a-1,M_a-M_b+\mu}(\mathbf{k})\\ &\times\left[\frac{\langle e_1\rangle}{m_1}\frac{(x^{(1)})^{L_a-1}\exp(-F^{(1)}k^2)}{D^{5/2}}\right.\\ &\left.+(-1)^{L_a}\frac{\langle e_2\rangle}{m_2}\frac{(x^{(2)})^{L_a-1}\exp(-F^{(2)}k^2)}{D^{5/2}}\right]\,, \end{aligned} \tag{18}$$

where we have introduced the usual notation $\hat{L_a}=\sqrt{2L_a+1}$. Note that this term vanishes if $L_a = 0$.

The term $\mathcal{M}_\mu(A;x)$ comes from the magnetic part of the operator and reads

$$\begin{aligned}\mathcal{M}_\mu(A;x) &= (-1)^{1+S_a}2\pi\Gamma(3/2)\hat{S_a}\begin{Bmatrix}1 & 1/2 & 1/2\\ 1/2 & S_a & J_b\end{Bmatrix}\\ &\times\left[\frac{\langle e_1\rangle}{m_1}\frac{x^{(1)\ L_a}\exp(-F^{(1)}k^2)}{D^{3/2}} + (-1)^{L_a+S_a+J_b}\frac{\langle e_2\rangle}{m_2}\right.\\ &\left.\times\frac{x^{(2)\ L_a}\exp(-F^{(2)}k^2)}{D^{3/2}}\right]\sum_{\mu_a,\sigma_a,\nu,\sigma}\langle L_a\mu_a S_a\sigma_a \mid J_aM_a\rangle\\ &\times\langle S_a\sigma_a 1\nu \mid J_bM_b\rangle\langle 1\nu 1\sigma \mid 1\mu\rangle\mathcal{Y}_{1\sigma}(\mathbf{k})\mathcal{Y}_{L_a\mu_a}(\mathbf{k})\,. \end{aligned} \tag{19}$$

The case $L_a = 0$ looks very similar, but one has to be very careful with the phases. In this case the electric part is given by

$$\mathcal{E}_\mu(B;z) = (-1)^{L_b-1-\mu}\mathcal{E}^*_{-\mu}(A = B; x = z)\,, \tag{20}$$

meaning that in expression (18), one has to replace all quantities relative to A by the corresponding ones relative to B, change the sign of μ, change x by z, take the complex conjugate and multiply by a given phase. The expression for $\mathcal{M}_\mu(B;z)$ is obtained with the same prescription as (20).

If one admits more than one Gaussian function in the expansion of the wave function the quantities defined in (15) depend on which terms are retained and must be written more explicitly, *i.e.*, $D_{ij} = (A_i + B_j)/2$. To obtain the complete expression corresponding to the exact wave function, one must take care of this; for example one must make in (18)-(19) the following replacement:

$$\begin{aligned}&\frac{(x^{(1)})^{L_a-1}\exp(-F^{(1)}k^2)}{D^{5/2}} \to\\ &\sum_{i,j=1}^{N} c_i^{\mathrm{A}}c_j^{\mathrm{B}}\frac{(x^{(1)}_{ij})^{L_a-1}\exp(-F^{(1)}_{ij}k^2)}{D^{5/2}_{ij}}\end{aligned} \tag{21}$$

and similar replacements everywhere.

Thus, with the prescription (6) for the wave function, the transition amplitudes can be calculated exactly, without any numerical integration.

4 The phase space

4.1 Density of states

The density of states is obtained with periodic conditions on the box. The treatment can be found in any textbook. The density of states per unit energy and per unit solid angle is given by

$$\rho(E,\Omega) = \frac{VE^2}{(2\pi)^3}\,. \tag{22}$$

One has to calculate the matrix element $\mid\langle B\gamma|H_i|A\rangle^2\mid$ from (7). The best way is to use spherical components for the vectors and Racah algebra to deal with the corresponding expressions. One has then to sum over the polarisations of the photon and of the final meson and to average over the polarisations of the decaying meson. In order to simplify the notation, let us introduce the quantity $X(E)$ by

$$X(E)\delta_{\mathbf{K}_b,-\mathbf{k}} = \frac{1}{\hat{J_{\mathrm{A}}}^2}\sum_{\lambda=\pm1}\sum_{M_a,M_b}\mid\langle B\gamma|H_i|A\rangle\mid^2\,. \tag{23}$$

The decay width is given by the golden rule:

$$\Gamma = \int \mathrm{d}E\ \delta(E_{\mathrm{f}} - E_{\mathrm{i}})\int \mathrm{d}\Omega\ 2\pi\ \rho(E,\Omega)X(E)\,. \tag{24}$$

In the literature, one finds different formulae for the width depending upon how the delta-distribution reflecting energy conservation is treated in (24). This is known as the phase space factor Φ. Explicitly, one writes the width as

$$\Gamma = \Phi(E_0) V X(E_0)\,. \tag{25}$$

As required, the box volume V, appearing in (25), cancels with the one present in $X(E)$ as seen from (7). E_0 denotes the photon energy value fulfilling the energy conservation equation $E_{\rm f} = E_{\rm i}$.

4.2 Relativistic phase space

In this case the energies $E_{\rm f}$ and $E_{\rm i}$ are given by their relativistic expressions. Taking into account the fact that the momentum of the final meson is opposite to the photon momentum, the Dirac factor is $\delta(E_{\rm B} + E - m_a) = \delta(\sqrt{m_b^2 + E^2} + E - m_a)$. The integral in (24) is performed with the usual rules on delta-functions to give

$$\Phi(E_0) = \frac{E_0^2}{\pi}\frac{E_{\rm B}(E_0)}{m_a}\,, \qquad E_0 = \frac{m_a^2 - m_b^2}{2m_a}\,. \tag{26}$$

4.3 Non-relativistic phase space

In a non-relativistic treatment, the energies are related to their momenta by the classical expressions. Alternatively, one can make the approximation $E_0 \ll m_a,\ m_b$ in the relativistic phase (26), leading to

$$\Phi(E_0) = \frac{E_0^2}{\pi}\,, \qquad E_0 = m_a - m_b\,. \tag{27}$$

Thus, compared to the relativistic expression, the non-relativistic phase space differs by two effects. The energy of the photon is equal to the energy difference between the resonances and the term $\frac{E_{\rm B}(E_0)}{m_a}$ is equal to unity.

This kind of phase space is traditional in atomic or in nuclear physics; it has no real justification when applied to meson decays. Nevertheless, it is still of common use. Sometimes in the literature [15] a mixed phase space based on (26) for E_0 and on (27) for $\Phi(E_0)$ is employed. We shall comment on those aspects later on.

5 Total widths

5.1 General case

We now come to the expression of the width in the general case, but with the wave functions expanded in Gaussian terms, as discussed previously. We present the results only in the case $L_b = 0$. The results for $L_a = 0$ are easily obtained from these ones with the correct replacement (20) and the modification due to spin average. We do not want to enter into too much detail because the calculations are known in nuclear physics and result directly from Racah algebra. We report the result below:

$$\Gamma_{\rm A\to B\gamma} = \delta_{S_b,J_b} 2\alpha \frac{E_{\rm B}(E_0)}{m_a}[\mathcal{EE} + \mathcal{EM} + \mathcal{MM}]\,. \tag{28}$$

The terms $\mathcal{EE}, \mathcal{EM}, \mathcal{MM}$ come from the electric-electric, electric-magnetic, magnetic-magnetic part in the square of the amplitude. One sees that a transition is no longer either of a purely electric or magnetic type, but a mixing of both with interference effects. They are given by

$$\begin{aligned}
\mathcal{EE} &= \delta_{S_a,S_b}\frac{\Gamma(5/2)^2}{36} L_a(L_a+1) k_0^{2L_a-1}\mathcal{A}^2\,,\\
\mathcal{EM} &= \delta_{S_a,S_b}(-1)^{L_a+S_a+J_a+J_b+1}\frac{\Gamma(3/2)\Gamma(5/2)}{2\sqrt{6}}\\
&\quad\times\sqrt{L_a(L_a+1)}\hat{S}_a\hat{L}_a\hat{J}_b \begin{Bmatrix} 1 & 1/2 & 1/2\\ 1/2 & S_a & J_b\end{Bmatrix}\\
&\quad\times\begin{Bmatrix} L_a & S_a & J_a\\ J_b & L_a & 1\end{Bmatrix} k_0^{2L_a+1}\mathcal{AB}\,,
\end{aligned} \tag{29}$$

$$\begin{aligned}
\mathcal{MM} &= \frac{3}{4}\Gamma(3/2)^2 \hat{S_a}^2\hat{L_a}^2\hat{J_b}^2 \begin{Bmatrix} 1 & 1/2 & 1/2\\ 1/2 & S_a & J_b\end{Bmatrix}^2\\
&\quad\times k_0^{2L_a+3}\mathcal{B}^2\sum_J \langle 1\ 1\ L_a\ 0 \mid J\ 1\rangle^2\\
&\quad\times\begin{Bmatrix} L_a & S_a & J_a\\ J_b & J & 1\end{Bmatrix}^2\,,
\end{aligned} \tag{30}$$

where the dynamical factors $\mathcal{A}$ and $\mathcal{B}$ result from the meson wave functions

$$\begin{aligned}
\mathcal{A} &= \sum_{i,j}\frac{c_i^{\rm A}c_j^{\rm B}}{D_{ij}^{5/2}}\left[\frac{\langle e_1\rangle}{m_1}(x_{ij}^{(1)})^{L_a-1}\exp(-F_{ij}^{(1)}k_0^2)\right.\\
&\quad\left.+(-1)^{L_a}\frac{\langle e_2\rangle}{m_2}(x_{ij}^{(2)})^{L_a-1}\exp(-F_{ij}^{(2)}k_0^2)\right]\,,
\end{aligned} \tag{31}$$

$$\begin{aligned}
\mathcal{B} &= \sum_{i,j}\frac{c_i^{\rm A}c_j^{\rm B}}{D_{ij}^{3/2}}\left[\frac{\langle e_1\rangle}{m_1}(x_{ij}^{(1)})^{L_a}\exp(-F_{ij}^{(1)}k_0^2)\right.\\
&\quad\left.+(-1)^{L_a+S_a+J_b}\frac{\langle e_2\rangle}{m_2}(x_{ij}^{(2)})^{L_a}\exp(-F_{ij}^{(2)}k_0^2)\right].
\end{aligned} \tag{32}$$

Let us remark that if $L_a = 0$ (transition from S state to S state), the terms $\mathcal{EE}$ and $\mathcal{EM}$ vanish, and the transition is purely magnetic. Now, we have in hand all the tools to perform exact calculations. The formulae may appear to be complicated but they simplify a lot for transitions of experimental interest.

6 The results

We want to stress again that, due to the fact that the wave functions have been determined with given potentials and that the transition operator is perfectly well defined, all the results presented in this section (except the very last subsection concerning mixing angles) are free from any adjustable parameter. They thus provide a very good tool for exploring in detail the drawbacks of the formalism.

Table 1. Comparison, with the use of AL1 potential, among the various approximations for the electric transitions (first column): long-wavelength approximation LWLA with non-relativistic phase space (second column) and relativistic phase space (fourth column), and dipole approximation DA with relativistic phase space (third column).

$^3S_1 \to {}^3P_J$					
Transition	$\phi_{\rm nrel}$, LWLA	$\phi_{\rm rel}$, DA	$\phi_{\rm rel}$, LWLA	Exact	Exp. (keV)
$\psi(2S) \to \chi_{c0}(1P)\gamma$	19.77	49.92	17.70	14.12	25.76 ± 3.81
$\psi(2S) \to \chi_{c1}(1P)\gamma$	38.40	43.43	35.75	34.25	24.10 ± 3.49
$\psi(2S) \to \chi_{c2}(1P)\gamma$	47.35	30.23	44.90	46.39	21.61 ± 3.28
$\Upsilon(2S) \to \chi_{b0}(1P)\gamma$	0.44	1.52	0.43	0.41	1.89 ± 0.53
$\Upsilon(2S) \to \chi_{b1}(1P)\gamma$	1.06	2.34	1.04	1.02	2.95 ± 0.61
$\Upsilon(2S) \to \chi_{b2}(1P)\gamma$	1.49	2.39	1.47	1.49	2.90 ± 0.61
$\Upsilon(3S) \to \chi_{b0}(2P)\gamma$	0.70	1.65	0.68	0.66	1.42 ± 0.25
$\Upsilon(3S) \to \chi_{b1}(2P)\gamma$	1.69	2.67	1.67	1.65	2.97 ± 0.43
$\Upsilon(3S) \to \chi_{b2}(2P)\gamma$	2.45	2.91	2.42	2.44	3.00 ± 0.45
$^3P_J \to {}^3S_1$					
Transition	$\phi_{\rm nrel}$, LWLA	$\phi_{\rm rel}$, DA	$\phi_{\rm rel}$, LWLA	Exact	Exp. (keV)
$f_1(1285) \to \rho^0\gamma$	1727.12	824.56	939.73	1232.83	1296.00 ± 295.20
$\chi_{c0}(1P) \to J/\psi(1S)\gamma$	268.67	144.59	233.40	255.40	92.40 ± 41.52
$\chi_{c1}(1P) \to J/\psi(1S)\gamma$	349.33	298.24	292.29	306.63	240.24 ± 40.73
$\chi_{c2}(1P) \to J/\psi(1S)\gamma$	387.90	396.53	319.01	262.05	270.00 ± 32.78
$\chi_{b0}(1P) \to \Upsilon(1S)\gamma$	30.63	20.36	28.82	30.10	seen
$\chi_{b1}(1P) \to \Upsilon(1S)\gamma$	33.14	25.59	31.03	31.51	seen
$\chi_{b2}(1P) \to \Upsilon(1S)\gamma$	34.67	29.14	32.37	30.39	seen
$\chi_{b0}(2P) \to \Upsilon(1S)\gamma$	13.58	11.32	12.12	14.01	seen
$\chi_{b0}(2P) \to \Upsilon(2S)\gamma$	13.47	9.37	13.07	13.31	seen
$\chi_{b1}(2P) \to \Upsilon(1S)\gamma$	13.99	12.30	12.45	13.53	seen
$\chi_{b1}(2P) \to \Upsilon(2S)\gamma$	14.97	12.77	14.47	14.51	seen
$\chi_{b2}(2P) \to \Upsilon(1S)\gamma$	14.22	12.89	12.63	11.80	seen
$\chi_{b2}(2P) \to \Upsilon(2S)\gamma$	15.82	15.04	15.27	14.63	seen

6.1 Influence of various approximations

In this section, we wish to indicate the effects of a number of approximations that can be found in earlier works.

As seen from fig. 2, there exists a sizeable difference if one uses a Gaussian-type wave function ($N = 1$ in the expansion (6) or the exact one $N = 5$). This effect of course appears in the results concerning the widths. Passing from $N = 1$ to $N = 2$ leads to a difference around 10%, from $N = 2$ to $N = 3$ one sees a further small difference around 1%, while for $N > 3$ the results are perfectly stable. This means that 3 Gaussian terms are sufficient to describe the wave function in a correct way. Nevertheless, for the rest of our study, every calculation is performed with $N = 5$ and the result is considered as the exact one concerning the wave function. This is particularly important in the case of radial excitations (with one or several nodes in the radial part), since obviously $N = 1$ cannot explain such a state and even $N = 2$ could be a crude approximation. Moreover, since our results are analytical, computation with $N = 5$ is practically as fast as the $N = 3$ case.

In table 1 we present the results concerning various approximations, with use of AL1 potential, for electric transitions (only electric transitions are concerned with dipole approximation). Let us discuss first the effect of phase space. Indeed, the use of experimental masses is fundamental to a good photon energy which is of primary importance in the formulae. A relativistic phase space always gives the right order of magnitude, whereas a non-relativistic one can be dramatically off. In table 1 this effect is moderate because it mainly deals with very heavy mesons but in the case of magnetic transitions, more common in the light meson sector, the effect can reach a factor 10 for some transitions (in $\rho \to \pi\gamma$ the non-relativistic phase space gives 547 keV, while the relativistic one gives 57 keV or $\omega \to \pi\gamma$ for which the corresponding values are, respectively, 5239 keV and 543 keV). In this case, the fault is partly due to an overestimation of the factor $E_{\rm B}/m_a$ which non-relativistically is taken to be unity (the value for $\rho \to \pi\gamma$ is 0.52). But the main problem comes essentially from an incorrect determination of the momentum $k_0 = E_0$, that enters both in the $\frac{E_{\rm B}}{m_A}$ factor and in the amplitudes. There exist some important discrepancies between the relativistic and the non-relativistic momenta, and this leads to very important effect on the width. A mixed phase space gives results in between. Among all the approximations that are commonly employed in nuclear physics, the use of a non-relativistic phase space is certainly the worse when applied to radiative transitions of mesons. The phase space is essentially a kinematical ingredient and, even if one uses a non-relativistic approximation for the wave function or for the quark-photon ver-

Table 2. General case, relativistic phase space, AL1, AP1, and DNR potentials. For those transitions, the electric and interference terms are null.

$^3S_1 \rightarrow {}^1S_0$				
Transition	Tot(AL1)	Tot(AP1)	Tot(DNR)	Exp. (keV)
$\rho^+ \rightarrow \pi^+\gamma$	48.48	60.41	44.64	67.82 ± 7.55
$\rho^0 \rightarrow \pi^0\gamma$	48.66	60.64	44.81	102.48 ± 25.69
$\rho^0 \rightarrow \eta\gamma$	47.73	60.63	51.53	36.18 ± 13.57
$\omega \rightarrow \pi^0\gamma$	459.30	571.79	423.19	714.85 ± 42.74
$\omega \rightarrow \eta\gamma$	6.08	7.72	6.56	5.47 ± 0.84
$\phi(1020) \rightarrow \eta\gamma$	41.27	44.12	31.95	55.82 ± 2.73
$\phi(1020) \rightarrow \eta'(958)\gamma$	0.30	0.32	0.27	0.53 ± 0.31
$\mathrm{K}^*(892)^0 \rightarrow \mathrm{K}^0\gamma$	98.28	116.41	85.93	116.15 ± 10.19
$\mathrm{K}^*(892)^+ \rightarrow \mathrm{K}^+\gamma$	79.07	104.46	66.99	50.29 ± 4.66
$\mathrm{D}^*(2007)^0 \rightarrow \mathrm{D}^0\gamma$	33.60	41.74	28.22	$< 800.10 \pm 60.90$
$\mathrm{D}^*(2010)^+ \rightarrow \mathrm{D}^+\gamma$	2.48	3.58	1.84	$< 1.44\ ^{+2.75}_{-0.92}$
$\mathrm{D}_\mathrm{s}^{*+} \rightarrow \mathrm{D}_\mathrm{s}^+\gamma$	0.26	0.31	0.18	$< 1789.80 \pm 47.50$
$\mathrm{B}^{*+} \rightarrow \mathrm{B}^+\gamma$	0.97	1.26	0.78	seen
$\mathrm{B}^{*0} \rightarrow \mathrm{B}^0\gamma$	0.28	0.36	0.23	seen
$J/\Psi \rightarrow \eta_c\gamma$	1.85	1.87	1.75	1.13 ± 0.35
$\psi(2S) \rightarrow \eta_c(1S)\gamma$	4.97	6.34	7.13	0.78 ± 0.19
$^1S_0 \rightarrow {}^3S_1$				
Transition	Tot(AL1)	Tot(AP1)	Tot(DNR)	Exp. (keV)
$\eta'(958) \rightarrow \rho^0\gamma$	112.90	143.62	107.50	61.31 ± 5.51
$\eta'(958) \rightarrow \omega\gamma$	10.50	13.36	10.01	6.11 ± 0.78

tex, it is absolutely necessary to take a relativistic phase space and an exact determination of the photon energy.

The dipole approximation (DA) is also widely used in atomic and nuclear physics for $E1$ transitions. It must be considered more as a convenient approximation (the matrix elements are simpler to calculate) than an approximation based on physical arguments. Nevertheless the effect is also important, although weaker than the phase space one, since it can attain a factor 3 in certain cases (see table 1). Sometimes it increases the results while in other cases it decreases them, so that it is not possible to draw reliable conclusions. We consider that DA should be avoided in the meson sector, although its effect is not really dramatic.

Lastly, the long-wavelength approximation (LWLA) is probably the approximation that is most commonly used. In this scheme, a number of transitions are completely forbidden, while they have been observed experimentally, some of them with an appreciable width. The approximation obviously fails in this case. For $^3P_J \rightarrow {}^3S_1$ or $^3S_1 \rightarrow {}^3P_J$ transitions, a correct treatment predicts electric-magnetic mixing, while LWLA does not allow this mixing. In such a situation LWLA can differ by more than 25% from the exact results (see table 1 and for example the case of $f_1 \rightarrow \rho_0\gamma$ transition).

For $L_a = L_b = 0$ only the magnetic term remains, while a pure electric term remains for $^1P_1 \rightarrow {}^1S_0$. In this case the LWLA gives always a larger value; this can be shown analytically if the wave function has only one Gaussian component. Since in general one component is dominant it is not surprising that this property persists even in more realistic situations. Although this is not always the case, LWLA often gives better (as compared to experiment) results; this means that either the wave functions are not so good or that something is still missing in the theory.

6.2 General study for three different quark-antiquark potentials

In this part we present the most sophisticated calculations in this framework. We go beyond LWLA, use relativistic phase space and exact wave functions. The aim is to test the three quark-antiquark potentials proposed in subsect. 2.1, to see whether the results are very sensitive to the dynamics of quarks inside a meson. The results are presented in tables 2-4.

The transitions $^1P_1 \rightarrow {}^3S_1$ and $^3P_J \rightarrow {}^1S_0$ are purely magnetic but are completely forbidden in LWLA. Our complete treatment predicts them with the right order of magnitude.

An overall look at those tables shows us the similarity of the decay widths resulting from the AL1, AP1 and DNR potentials. The results obtained with AL1 generally lie between those of DNR and AP1. The predicted values coming from the AL1 potential are smaller than the AP1 ones. This could be related to the different asymptotic behavior of the potential at long range. The confinement being less steep in the AP1 potential, the spread of the wave function is more important and contributes more to the spatial integration. Globally, no potential is obviously more suited than the others for those calculations. DNR

Table 3. Same as table 2 except that the electric, magnetic and interference terms contribute to the width. The columns number 2, 3 and 4 refer to the DNR potential.

$^3S_1 \to {}^3P_J$							
Transition	Elec.	Interfer.	Magn.	Tot(AL1)	Tot(AP1)	Tot(DNR)	Exp. (keV)
$\psi(2S) \to \chi_{c0}(1P)\gamma$	22.48	−4.15	0.19	14.12	14.06	18.52	25.76 ± 3.81
$\psi(2S) \to \chi_{c1}(1P)\gamma$	45.14	−1.83	0.04	34.25	34.23	43.34	24.10 ± 3.49
$\psi(2S) \to \chi_{c2}(1P)\gamma$	56.58	1.28	0.02	46.39	46.43	57.88	21.61 ± 3.28
$\Upsilon(2S) \to \chi_{b0}(1P)\gamma$	0.86	−0.03	0.00	0.41	0.54	0.82	1.89 ± 0.53
$\Upsilon(2S) \to \chi_{b1}(1P)\gamma$	2.06	−0.02	0.00	1.02	1.35	2.04	2.95 ± 0.61
$\Upsilon(2S) \to \chi_{b2}(1P)\gamma$	2.92	0.02	0.00	1.49	1.97	2.94	2.90 ± 0.61
$\Upsilon(3S) \to \chi_{b0}(2P)\gamma$	1.12	−0.03	0.00	0.66	0.73	1.09	1.42 ± 0.25
$\Upsilon(3S) \to \chi_{b1}(2P)\gamma$	2.73	−0.02	0.00	1.65	1.84	2.71	2.97 ± 0.43
$\Upsilon(3S) \to \chi_{b2}(2P)\gamma$	3.96	0.03	0.00	2.44	2.71	3.98	3.00 ± 0.45
$^3P_J \to {}^3S_1$							
Transition	Elec.	Interfer.	Magn.	Tot(AL1)	Tot(AP1)	Tot(DNR)	Exp. (keV)
$f_1(1285) \to \rho^0\gamma$	718.41	354.45	87.44	1232.83	1376.96	1160.31	1296.00 ± 295.20
$\chi_{c0}(1P) \to J/\psi(1S)\gamma$	237.70	29.16	0.89	255.40	260.24	267.75	92.40 ± 41.52
$\chi_{c1}(1P) \to J/\psi(1S)\gamma$	291.39	29.39	1.48	306.63	312.43	322.27	240.24 ± 40.73
$\chi_{c2}(1P) \to J/\psi(1S)\gamma$	314.28	−38.59	3.32	262.05	266.99	279.01	270.00 ± 32.78
$\chi_{b0}(1P) \to \Upsilon(1S)\gamma$	28.02	2.01	0.04	30.10	30.85	30.06	seen
$\chi_{b1}(1P) \to \Upsilon(1S)\gamma$	30.07	1.26	0.03	31.51	32.26	31.35	seen
$\chi_{b2}(1P) \to \Upsilon(1S)\gamma$	31.30	−1.43	0.05	30.39	31.03	29.91	seen
$\chi_{b0}(2P) \to \Upsilon(1S)\gamma$	7.01	1.02	0.04	14.01	11.80	8.07	seen
$\chi_{b0}(2P) \to \Upsilon(2S)\gamma$	14.01	0.49	0.00	13.31	13.52	14.50	seen
$\chi_{b1}(2P) \to \Upsilon(1S)\gamma$	7.21	0.56	0.02	13.53	11.38	7.80	seen
$\chi_{b1}(2P) \to \Upsilon(2S)\gamma$	15.45	0.33	0.00	14.51	14.72	15.79	seen
$\chi_{b2}(2P) \to \Upsilon(1S)\gamma$	7.33	−0.59	0.03	11.80	9.90	6.78	seen
$\chi_{b2}(2P) \to \Upsilon(2S)\gamma$	16.28	−0.39	0.01	14.63	14.82	15.89	seen

Table 4. Same as table 2. The transition $^1P_1 \to {}^1S_0$ is electric whereas the two other types are purely magnetic.

$^1P_1 \to {}^1S_0$				
Transition	Tot(AL1)	Tot(AP1)	Tot(DNR)	Exp. (keV)
$b_1(1235)^+ \to \pi^+\gamma$	148.68	152.76	118.27	227.20 ± 58.60
$^3P_J \to {}^1S_0$				
Transition	Tot(AL1)	Tot(AP1)	Tot(DNR)	Exp. (keV)
$a_1(1260)^+ \to \pi^+\gamma$	179.53	229.90	171.45	seen
$a_1(1260)^0 \to \pi^0\gamma$	–	–	–	seen
$a_2(1320)^+ \to \pi^+\gamma$	142.01	179.27	136.64	299.60 ± 65.71
$^1P_1 \to {}^3S_1$				
Transition	Tot(AL1)	Tot(AP1)	Tot(DNR)	Exp. (keV)
$D_{s1}(2536)^{*+} \to D_s^{*+}\gamma$	10.97	11.99	8.63	probably seen

gives better results in heavy mesons in general, while AP1 seems better for $L_a = L_b = 0$ transitions and AL1 for dominant electric transitions.

The trends are essentially the same and when one potential gives too low (or too high) a value, so do the others. The agreement with experiment is satisfactory for all types of transitions, giving indication that we are on the right track for the description of mesons. The discrepancy with experiment very rarely exceeds 50% and this can be considered as encouraging owing to the fact that we have no free parameters. However, the results are not completely satisfactory. It is very difficult to compare our work with previous ones, because very few authors attempted to use a unified treatment for the totality of the transitions. A notable exception is the extensive study of Godfrey and Isgur [17]; we obtain results of the same quality. Very often, Godfrey and Isgur obtained too high values, whereas our wave functions tend to underestimate the data. However, we have no free parameters, while they have two free parameters for fitting the transitions and they used an *ad hoc* phase space factor, which seems to us quite artificial.

The fact that three different realistic wave functions, based on potentials that nicely reproduce the spectra, give more or less the same trends (although there can exist

20% differences) shows that the quality of the wave function is not responsible entirely for the discrepancy with experiment. This is not often the case (except of course when it gives a null result). This proves that something is still missing in the formalism although current calculations provide the dominant contributions.

Now let us have a closer look to some interesting transitions. A special one concerns the neutral and charged decays of the ρ into the $\pi\gamma$. Experimentally the decay width for the charged channel is 68 keV, whereas the measured value for the neutral channel is 102 keV. In our calculation the small difference between these two channels comes only from the tiny difference between the experimental masses of the π^+ and the π^0. The decay width has the same expression for both transitions due to the term $\left[\frac{\langle e_1\rangle}{m_1} - \frac{\langle e_2\rangle}{m_2}\right]^2$ in expression (19) appearing for mesons composed of a single flavor. That is $\left[\frac{2}{3} - \frac{1}{3}\right]^2 = \frac{1}{9}$ for the charged channel and $\left[\frac{1}{6} - \frac{-1}{6}\right]^2 = \frac{1}{9}$ for the neutral one. So where does this important variation between those two channels come from? First we have to point out that given the large uncertainties 67.82±7.55 and 102.48±25.69 the two values are nearly compatible with 76 MeV. This means that there may be no problem with those channels except an experimental one! Nevertheless if we rely on the experimental values, a possible explanation could come from the $\omega \to \pi^0\gamma$ transition, which is identical with $\rho^0 \to \pi^0\gamma$ but with an enhancement of a factor of 9 due to isospin. The experimental value 715 keV is roughly in agreement with this point. So even a small isospin mixing between the ω and the ρ^0 could sufficiently increase the decay width to explain the data. This hypothesis will be tested in the next section.

We remark the same variation for the K* decaying into the K-meson and for the B* into the B. However, in this case the isospin factor explains this variation. It appears as a factor $(\frac{1}{3m_n} + \frac{1}{3m_s})^2$ for the neutral channel and a factor $(\frac{2}{3m_n} - \frac{1}{3m_s})^2$ for the charged one in the LWLA (it is more complicated to estimate the ratio of the strange with the isospin doublet masses in the general formalism). Using the experimental data and making the approximation that the matrix elements in those two channels are identical (except for the isospin dependence), we find the relation: $m_s = 1.24 m_n$. In our potentials this ratio $\frac{m_s}{m_n}$ is 1.83, 1.78, 1.78 for the AL1, AP1 and DNR, respectively.

Concerning the transition $a_1^0 \to \pi^0\gamma$, the decay width is zero; this is due to the fact that for the ${}^3P_J \to {}^1S_0$ composed of a single flavor the width is proportional to $\left[\frac{\langle e_1\rangle}{m_1} + \frac{\langle e_2\rangle}{m_2}\right] = 0$.
In the potentials used, there is no isospin dependence for $S = 1$ states, so the ρ, ω have the same radial part in the wave function; the same remark is true for the π and η_n for AL1 and AP1 (no instanton effect) while DNR in principle gives a good description of η and η' resonances. Nevertheless, even for transitions involving those resonances, DNR is not systematically superior, showing again that the quality of the wave functions is not the only crucial ingredient of the formalism. It is not sure that the decay of the $D_{s1}(2536)^{*+}$ into $D_s^*\gamma$ has been observed experimentaly but our result for this width suggests that it should be seen experimentally.

6.3 Mixing angles

If the wave function is composed of two parts as in the η-mesons (flavor mixing), or in the ρ (isospin mixing with the ω), further extensions are needed in the formalism. In the case of η, the wave function can be written: $|\Psi_\eta\rangle = |\Psi_{\eta_n}(n\bar{n}; I = 0)\rangle - |\Psi_{\eta_s}\rangle$. In our study when no instanton effect is present (AL1 and AP1), we introduce (by hand) a mixing of 50% between the two flavors. That is we calculate separately the states $\tilde{\eta}_n$ a nd $\tilde{\eta}_s$ both normalised to unity and we have $|\Psi_{\eta_n}(n\bar{n}; I = 0)\rangle = \frac{\tilde{\eta}_n}{\sqrt{2}}$, $|\Psi_{\eta_s}\rangle = \frac{\tilde{\eta}_s}{\sqrt{2}}$. A possible difficulty is that those states do not have the same mass in order to calculate the phase space; nevertheless as we take the experimental value this difficulty is avoided. In the case of DNR there is no ambiguity and the percentage of each channels is given dynamically (around 55% for the ordinary sector and 45 % for the strange sector in the case of η-resonance).
From a general point of view we write $|\Psi\rangle = |\Psi_1\rangle \pm |\Psi_2\rangle$, where 1 and 2 denote the two flavor (or isospin) components of the wave function. We have to calculate

$$M(\mathrm{A} \to \mathrm{B}\gamma) = \langle A|\mathbf{M}|B\rangle = (\langle A_1| \pm \langle A_2|)\mathbf{M}(|B_1\rangle \pm |B_2\rangle)\,, \qquad (33)$$

so there could exist 4 components, and therefore some interferences. In the case of flavor mixing not all the terms will contribute due to flavor conservation.

As we will see in subsects. 6.3.1 and 6.3.2, the ϕ could decay into the ω, the ρ and the π. This could be incorporated to our decay process by two ways: an isospin mixing (ω and ρ) or a flavor mixing (ϕ and ω). The study of this problem was carried out with the general formalism and a relativistic phase space. Because of the similarity of the results obtained via the three potentials, and just as a matter for comparison, it is sufficient to perform the calculation only with AL1 and DNR potentials.

Concerning the η and η' resonances, the wave functions resulting from the AL1 and AP1 potentials need a flavour mixing angle inserted by hand, such as in (2), while the DNR potential provides this mixing in a natural and dynamical way.

Some other comments are in order. The QED conserves the flavor of the particles at the vertex (the radiative transitions with flavor change $b \to s\gamma$ have been intensively studied recently [18,16] but they need penguin diagrams that we do not consider here); this implies that the quark content of meson B is the same as the one in the initial meson A (in our elementary decay process exhibited in fig. 3). Nevertheless the experimental data show a non-zero decay width for the following transitions concerning vector mesons: $\phi \to \omega\gamma$ and $\phi \to \rho\gamma$. For a ϕ-meson taken to be a pure $s\bar{s}$, as usually prescribed, this seems to indicate that flavor conservation is violated. Instanton effects cannot be invoqued because they do not play any role for a

Table 5. Decay widths obtained with a mixing angle of $\theta_f = 4.48^\circ$ between the ϕ and ω mesons for the AL1 potential and $\theta_f = 4.64^\circ$ for the DNR one. Beyond the long-wavelength approximation, relativistic phase space. The mixing angle is obtained from the $\phi \to \pi^0\gamma$.

$^3S_1 \to {}^1S_0$					
Transition	k_0	$\frac{E_B}{m_A}$	AL1	DNR	Exp. (keV)
$\omega \to \pi^0\gamma$	380	0.51	456.49	420.42	714.85 ± 42.74
$\omega \to \eta\gamma$	200	0.74	7.22	7.62	5.47 ± 0.84
$\phi(1020) \to \pi^0\gamma$	501	0.51	fitted	fitted	5.617 ± 0.447
$\phi(1020) \to \eta\gamma$	363	0.64	35.88	26.92	55.82 ± 2.73
$\phi(1020) \to \eta'(958)\gamma$	60	0.94	0.34	0.31	0.53 ± 0.31
$^1S_0 \to {}^3S_1$					
Transition	k_0	$\frac{E_B}{m_A}$	AL1	DNR	Exp. (keV)
$\eta'(958) \to \omega\gamma$	159	0.83	8.58	8.16	6.11 ± 0.78
$^3P_J \to {}^3S_1$					
Transition	k_0	$\frac{E_B}{m_A}$	AL1	DNR	Exp. (keV)
$f_1(1285) \to \phi\gamma$	236	0.82	0.48	0.50	17.76 ± 6.30
$^3S_1 \to {}^3P_J$					
$\phi \to f_0(980)\gamma$	39	0.96	0.03	0.03	1.52 ± 0.18
$\phi \to a_0(980)\gamma$	34	0.97	0.23	0.24	< 22.29

spin triplet. Those reactions result from more complicated processes. One can imagine for instance an annihilation of the $q\bar{q}$ pair in meson A into one or several virtual gluons and creation of a new $q\bar{q}$ pair in meson B (of possibly different flavor) that interact and emit a real photon. This is possible only for neutral flavor mesons. Indeed such transitions (with change of flavor) do not occur in kaons for example.

A possible way to take into account phenomenologically these kinds of transitions, in our elementary process, is to include in the wave functions of the ω a strange flavor componant, or/and in the ϕ wave function an n flavor part. A difficulty immediately appears in the case of the ρ resonance since it is isovector, while a strange flavor can only create an isoscalar. For the ω and ϕ one could introduce a mixing flavor angle θ_f. The physical mesons are now a combination of the ideal $\phi_0 = s\bar{s}$ and $\omega_0 = (n\bar{n})_{I=0}$:

$$\begin{pmatrix} \omega \\ \phi \end{pmatrix} = \begin{pmatrix} \cos\theta_f & \sin\theta_f \\ -\sin\theta_f & \cos\theta_f \end{pmatrix} \begin{pmatrix} \omega_0 \\ \phi_0 \end{pmatrix}.$$

With this modification, the transition $\phi \to \omega\gamma$ can be understood as the result of two contributions: $\phi(s\bar{s}) \to \omega(s\bar{s})\gamma$ and $\phi(n\bar{n}) \to \omega(n\bar{n})\gamma$. For the $\phi \to \rho\gamma$ only the n flavor part of the ϕ contributes.

From the electromagnetic point of view, only the charge is conserved, that is the projection of the isospin but not the isospin value. We can imagine an isospin mixing angle θ_I between neutral ρ and ω. As a consequence ρ couples to ϕ in second order. Another evidence for this possible mixing angle is the discrepancy between the neutral and charged channel of the $\rho \to \pi\gamma$. This isospin mixing could be understood by the near degeneracy of ρ and ω masses [31]:

$$\begin{pmatrix} \rho \\ \omega \end{pmatrix} = \begin{pmatrix} \cos\theta_I & \sin\theta_I \\ -\sin\theta_I & \cos\theta_I \end{pmatrix} \begin{pmatrix} \rho_0(I=1) \\ \omega_0(I=0) \end{pmatrix}.$$

Our mixing angles are chosen in order to recover the usual prescription for $\theta = 0$; this does not correspond always to the procedure used elsewhere.

6.3.1 Flavor mixing

In this subsection, we investigate the mixing between the ϕ and the ω. Technically we use the prescription of subsect. 6.3. We need to find an appropriate value for the mixing angle θ_f and, for that, we rely on experimental data. A good candidate is the transition $\phi \to \pi^0\gamma$ which exists only through a flavor mixing. Only the $n\bar{n}$ flavor part of the ϕ contributes to the decay. We find a small mixing of $\theta_f = 4.5$ degrees for AL1 and $\theta_f = 4.6$ for DNR. We could have chosen $\omega \to \eta\gamma$ to determine the angle value but the transition including an η-meson are not very appropriate because of its flavor mixing which could generate some interference terms. The $\omega \to \pi^0\gamma$ transition is also not well suited for this purpose, even if only one term ($\omega_{n\bar{n}}$) contributes because the value of a pure $n\bar{n}$ meson is smaller (459.30 keV) than the experimental value (714.85 keV) so that including a $s\bar{s}$ part in the ω which will not contribute to the decay could only decrease the width. The transitions modified in consequence are presented in table 5. Some transitions, seen experimentally, are forbidden without the mixing angle. They acquire a width but the effect is far from being sufficient. Concerning non-vanishing transitions, the effect is still too weak and very often in the wrong direction, showing that

Table 6. Decay widths obtained with a mixing angle of $\theta = 8.88^\circ$ between the ρ and ω mesons for the AL1 potential and $\theta = 10.13^\circ$ for the DNR one. Beyond the long-wavelength approximation, relativistic phase space. the determination of the mixing angle is based on the transition $\rho^0 \to \pi^0\gamma$.

$^3S_1 \to {}^1S_0$					
Transition	k_0	$\frac{E_B}{m_A}$	AL1	DNR	Exp. (keV)
$\rho^0 \to \pi^0\gamma$	373	0.52	fitted	fitted	102.48 ± 25.69
$\rho^0 \to \eta\gamma$	190	0.75	51.57	56.06	36.18 ± 13.57
$\omega \to \pi^0\gamma$	380	0.51	402.85	362.69	714.85 ± 42.74
$\omega \to \eta\gamma$	200	0.74	1.68	1.37	5.47 ± 0.84
$^1S_0 \to {}^3S_1$					
Transition	k_0	$\frac{E_B}{m_A}$	AL1	DNR	Exp. (keV)
$\eta'(958) \to \rho^0\gamma$	170	0.82	121.99	116.95	61.31 ± 5.51
$\eta'(958) \to \omega\gamma$	159	0.83	2.89	2.09	6.11 ± 0.78
$^3P_J \to {}^3S_1$					
Transition	k_0	$\frac{E_B}{m_A}$	AL1	DNR	Exp. (keV)
$f_1(1285) \to \rho^0\gamma$	410	0.68	1332.09	1262.35	1296.00 ± 295.20

a mixing angle is not able alone to explain completely the discrepancies.

6.3.2 Isospin mixing

Here we consider an isospin mixing between the ω and the ρ^0. This mixing does not appear for the charged $\rho^\pm$ because it is an $M_I = \pm 1$ meson. The angle $\theta_I = 8.9^\circ$ for AL1 and $\theta_I = 10.1^\circ$ for DNR are taken to fit the transition $\rho^0 \to \pi^0\gamma$, and discriminates between charged and neutral transitions. The results are presented in table 6.

Considering the poor quality of the results (4 transitions are deteriorated and 2 improved but still not reproducing the experimental values), it is clear that we are missing something. This could very well be a wrong angle value. Perhaps the $\rho^0 \to \pi^0\gamma$ transition results from another process and should not be used to determine θ_I.

7 Summary

This work is an exhaustive review of the decay of a meson into another one plus a real photon in a non-relativistic quark model. We have analyzed carefully the different parts of this elementary process. We discussed briefly various approximations that are widely used in literature *i.e.*, long-wavelength approximation, dipole approximation, different types of phase space factors. We showed that a relativistic phase space is the only important ingredient to obtain the correct order of magnitude for transition widths. The dipole approximation has no severe effect but could be easily avoided with the present-day computational facilities. The present treatment uses none of these approximations and allows the calculation of electric-magnetic interference terms and transitions forbidden in the LWLA and DA such as $^1S_0 \to^3 P_J$. We checked the importance of the wave function through the use of three potentials: AL1, AP1 and DNR. The last one takes care of instanton-induced effects and a finite size for the quark and should be considered as the "most realistic"; in particular it reproduces quite nicely the η and η' resonances. Nevertheless, the calculations do not reveal the superiority of any one of them, the predicted values being of the similar quality for all three potentials. DNR wave functions are better in the heavy-quark sectors, while AL1 and AP1 are to be preferred in the light-quark sectors. To obtain analytical results, we expanded our wave functions as a sum of N Gaussian terms. We found that $N = 3$ is sufficient to obtain a convergence of the results but in order to be sure to treat the exact wave function, we used everywhere in our calculation $N = 5$. We also showed that using exact wave functions is always preferable to the single Gaussian approximation that is in common use. The discrepancies can be as large as a 20%.

Finally we incorporated mixing angles in order to calculate some otherwise badly reproduced or even forbidden transitions such as $\phi \to \pi^0\gamma$. Those angles are of two kinds: isospin mixing between the ρ and ω mesons and flavor mixing between the ϕ and ω mesons. The results are not satisfactory. Except for a possible explanation of the important difference between neutral and charged decay of the ρ into π, the isospin mixing deteriorates the quality of the predicted values and the introduction of flavor mixing does not lead to important improvements.

Although a completely rigourous formalism gives an overall satisfactory agreement with experimental data, especially owing to the fact that we have no free parameters at our disposal, we gave arguments that, in the framework that we considered (NRQM and NR expression for the transition operator) some physics is still absent. We think that one can explore two different directions: inclusion of relativistic effects both in the wave functions and in the transition operator, and introduction of form factors at the quark-photon vertex. Work along these lines is in progress.

We are very grateful to Dr B. Desplanques for interesting discussions, and to L.A. Blanco for drawing our attention to important aspects concerning this work. We are very indebted to J. Cole for a careful reading of this manuscript.

References

1. N. Isgur, G. Karl, Phys. Rev. D **18**, 4187 (1978); **19**, 2653 (1979); **20**, 1191 (1979).
2. C. Semay, B. Silvestre-Brac, Phys. Rev. D **46**, 5177 (1992).
3. C. Semay, B. Silvestre-Brac, Nucl. Phys. A **618**, 455 (1997).
4. C. Semay, B. Silvestre-Brac, Nucl. Phys. A **647**, 72 (1999).
5. L.A. Copley, G. Karl, E. Obryk, Phys. Lett. B **29**, 177 (1969); Nucl. Phys. B **13**, 303 (1969).
6. P. Singer, Phys. Rev. D **1**, 86 (1970).
7. L.M. Brown, P. Singer, Phys. Rev. D **15**, 3484 (1977).
8. P. Hays, M.V.K. Ulehla, Phys. Rev. D **13**, 1339 (1976).
9. R.H Hackman, N.G. Deshpande, D.A. Dicus, V.L. Teplitz Phys. Rev. D **18**, 2537 (1978).
10. P.K. Chatley, C.P Singh, M.P. Khanna Phys. Rev D **29**, 96 (1984).
11. P.J. O'Donnell, Rev. Mod. Phys. **53**, 673 (1981).
12. T. Barnes, Phys. Lett. B **63**, 65 (1976).
13. E. Eichten, K. Gottfried, T. Kinoshita, K.D. Lane, J.M. Yan, Phys. Rev. D **17**, 3090 (1978); **21**, 203 (1980).
14. R. Mc Clary, N. Byers, Phys. Rev. D **28**, 1692 (1983).
15. N. Barik, P.C. Dash, A.R Panda, Phys. Rev. D **46**, 3856 (1992).
16. N. Barik, S. Kar, P.C. Dash, Phys. Rev. D **57**, 405 (1998).
17. S. Godfrey, N. Isgur, Phys. Rev. D **32**, 189 (1985).
18. El hassan El aaoud, Riazuddin, Phys. Rev. D **47**, 1026 (1993).
19. L.P. Fulcher, Phys. Rev. D **50**, 447 (1994).
20. C. Semay, R. Ceuleneer, B. Silvestre-Brac, J. Math. Phys. **34**, 2215 (1993).
21. D. Flam, F. Schöberl, *Introduction to the Quark Model of Elementary Particles* (Gordon and Breach Science Publishers, 1982).
22. B. Itzykson, J-B. Zuber, *Quantum Field Theory* (McGraw-Hill, 1980).
23. J. Carbonell, B. Desplanques, V.A. Karmanov, J.F. Mathiot, Phys. Rep. **300**, 215 (1998).
24. P.C. Tiemeijer, J.A. Tjon, Phys Lett B **277**, 38 (1992).
25. R. Ricken, M. Koll, D. Merten, B.C. Metsch, H.R. Petry, Eur. Phys. J. A **9**, 221 (2000).
26. B. Silvestre-Brac, C Semay, ISN **93-69** (unpublished); B. Silvestre-Brac, Few-Body Syst. **20**, 1 (1996); C. Semay, B. Silvestre-Brac, Z. Phys. C **61**, 271 (1994).
27. R.K. Bhaduri, L.E. Cohler, Y. Nogami, Nuovo Cimento A **65**, 376 (1981).
28. S. Ono, F. Schöberl, Phys. Lett. B **118**, 419 (1982).
29. W.H. Blask *et al.*, Z. Phys. A **337**, 327 (1990).
30. D.A. Varshalovich *et al.*, *Quantum Theory of Angular Momentum* (World Scientific, 1988).
31. A.R. Panda, K.C. Roy, Int. J. Mod. Phys. E **6**, 121 (1997).